Catalysis Today 176 (2011) 286–291

Contents lists available at ScienceDirect

Catalysis Today

journal homepage: www.elsevier.com/locate/cattod

Catalytic activity of Co–Mg mixed oxides in the VOC oxidation: Effects of ultrasonic assisted in the synthesis

Alejandro Pérez[a], Jean-François Lamonier[b], Jean-Marc Giraudon[b], Rafael Molina[a], Sonia Moreno[a,*]

[a] Estado Sólido y Catálisis Ambiental (ESCA), Departamento de Química, Facultad de Ciencias, Universidad Nacional de Colombia, AK 30 No. 45-03, Bogotá, Colombia
[b] Univ Lille Nord de France, Université de Lille 1, Unité de Catalyse et Chimie du Solide UMR CNRS 8181, 59650 Villeneuve d'Ascq, France

ARTICLE INFO

Article history:
Received 30 September 2010
Received in revised form
21 November 2010
Accepted 30 November 2010
Available online 6 January 2011

Keywords:
Ultrasound
Hydrotalcite
Mixed oxide
Butanol oxidation
VOCs

ABSTRACT

Ultrasound effect in the synthesis of catalysts of cobalt oxides prepared starting from the coprecipitation method of a hydrotalcite structure was evaluated in this work and characterized by DRX, FRX, BET, TPR and TPO. It is found that catalytic conversion of butanol on the Co–Mg–Al mixed oxides prepared by ultrasound method (10 min) is higher than that on the Co–Mg–Al mixed oxides prepared by conventional treatment (24 h). The surface area and the butanol oxidation are linearly related to the content of the hydrotalcite-like phase in the precursor, which resulted in highly dispersed Co (Co^{2+}), MgO and $A1_2O_3$ particles in the final catalyst. Similarly, the use of ultrasound in the synthesis reveals a benefic effect in so far as similar solids are obtained in much less time. The catalysts show greater activity and selectivity to CO_2 and H_2O than the commercial ones.

1. Introduction

Volatile organic compounds (VOCs) are important group of air pollutants. VOCs include any organic compound present in the atmosphere. Vehicle emissions, power generation and solvents emissions are considered to be the major sources of VOCs [1,2]. The term VOCs encompasses all the volatile organic compounds capable of producing photochemical oxidants by means of reactions provoked by solar light, in the presence of nitrate oxides [3].

Nowadays, the majority of the industrialized countries have incorporated measures of control through legislation which would tend to limit the environmental impact and the risks that these compounds might occasion on human health. In order to reduce the VOCs a series of technologies are proposed that could be applied in accordance with the diverse concentrations, categories and sources of contaminants [3,4].

Thermal combustion and reversible physical processes are beneficial when the concentration of the contaminant is relatively high. On the contrary, catalytic oxidation is the best option to eliminate organic compounds present in the gaseous phase in very low concentrations. The presence of a catalyst permits working at lower temperatures than those employed in thermal oxidation (between 350 and 400 °C), which represents an important economic benefit [5,6].

Numerous works evaluate the behaviour of some catalysts, among others, those based in noble metals (Au, Pt, Pd) [7–9] and transition metals, particularly Cu [2], Co [10], Fe, Mn [5,11–13] among others; these latter ones having the additional advantage of having a lower cost and a greater thermal resistance. However, their limited activity at low temperatures does not make them competitive in comparison with noble metal catalysts.

In order to overcome this inconvenience it is necessary to design catalysts in which the formation of highly dispersed metallic species is favoured, that improve the catalytic properties and prolong the useful life of the catalysts. Hydrotalcites are presented as precursors of mixed oxides, with an enormous potential for the generation of well dispersed, active and very stable catalysts.

These materials have motivated a great interest in catalysis as anion interchangers [5,13], catalytic supports and because of their basic properties, they have been employed in aldol condensation reactions [14,15] methanol synthesis [16], dehydrogenation of isopropanol, dehydrogenation of alkenes [17,18] among others.

Also, the interest in the application of calcined hydrotalcites (oxides) as catalysts in the environmental field is very important. For example, the materials resulting from the calcination of hydrotalcites based on copper and/or cobalt are very active and selective in the decomposition reaction of nitrogen oxides [19–21] as well as in the decomposition of sulphur oxides [22,23]. When transition metals are incorporated within the hydrotalcite structure, materials are obtained which are used equally as catalysts or as catalytic supports in redox reactions such as the selective oxida-

* Corresponding author. Tel.: +57 1 3165000; fax: +57 1 3165220.
E-mail address: smorenog@unal.edu.co (S. Moreno).

0920-5861/$ – see front matter © 2010 Elsevier B.V. All rights reserved.
doi:10.1016/j.cattod.2010.11.088

tion of hydrocarbons and in the total oxidation reactions of volatile organic compounds [5,24–27].

The catalytic activity of the hydrotalcites depends essentially on the M^{2+}/M^{3+} ratio, on the different cations that make up the network, on the nature of the compensation anions, and among others on the activation temperature [5,27].

The ultrasound (US) was used to increase the metallic dispersion and to allow a considerable decrease the time in the modification process without deterioration of the final material properties. Mg–Al hydrotalcite prepared under sonication presented an increase in the specific surface area and the number of defect sites in the solid, leading to a higher basicity [18,28,29].

In this work, Co hydrotalcites using ultrasound as an aging method were synthesized as precursors of the mixed oxides to butanol total oxidation.

2. Experimental

2.1. Synthesis of catalysts

The synthesis of Co hydrotalcites was obtained using the simultaneous co-precipitation technique (conventional treatment CT) at a constant pH [30], a solutions of $Mg(NO_3)_2{\cdot}6H_2O$ (Fluka, >99%), $Co(NO_3)_2{\cdot}6H_2O$ (Panreac >99%) and $Al(NO_3)_3{\cdot}9H_2O$ (Panreac, 98%) were mixed in a 3:1 molar ratio M^{2+}/M^{3+}. This solution was added dropwise to 0.2 M K_2CO_3 (Panreac, 99%) solution under vigorous stirring at 333 K. The pH was kept at 10 through addition of appropriate quantities of 1.5 M NaOH (Prolabo, 98%) solution, the precipitate obtained were aged for 24 h.

For the samples prepared under ultrasound (US), the solution with the precipitate is aged for 10 min under the ultrasound effect maintaining a frequency of 50 kHz (ultrasound bath Unique, model Ultracleaner 14000). This procedure was carried out at room temperature, and the gels obtained were not aged.

The precipitate was then separated by high-speed centrifugation, washed in deionized water to remove the alkali metals and nitrate ions until pH 7 was reached, and dried in oven at 353 K for 12 h. The resulting hydrotalcite were calcined at 723 for 16 h to obtain the mixed oxide (MO).

2.2. Characterization

The X-ray diffraction was carried out with a SHIMADZU LAB-X XRD-6000 difractometer with a Cu anode ($\lambda = 1.54056$ Å), using a step size of 0.02° 2θ and a velocity of 1° min^{-1}. TPR-H_2 profiles were taken by means of a CHEMBET 3000 (QUANTACHROME) equipment fitted with a thermal conductivity detector, following already reported methodologies. The samples (<250 μm) were previously degasified at 400 °C for 1 h in Ar and reduced with a heating ramp of 10 °C/min using 10% (v/v) H_2/Ar at 0.38 mL/s. The TPO analysis was carried out using Micromeritics Autochem 2920 equipment. Before proceeding with the oxidation, the samples were pre-reduced to 400 °C with a H_2 of 10 mL/min current for 2 h. The BET specific surface areas were measured by nitrogen adsorption at 77 K using an automatic volumetric apparatus (Micromeritics ASAP 2020). Samples were previously degassed for 8 h at 473 K and 10^{-3} Torr.

2.3. Catalytic evaluation

The solids were evaluated in the catalytic oxidation of butanol which is an alcohol representative of oxygenated VOCs and together with ethyl acetate, constitutes one of the principal components of the effluent gases which come from the printing of flexible material industry. For the catalytic evaluation a fixed bed reactor at atmospheric pressure was used, and the conversion was evaluated according to the temperature. 200 mg of catalyst and a total flow of 100 mL/min with a VOC concentration of 1000 ppm were used.

Prior to all catalytic tests, the samples were heated in a flowing in air (10 mL/min) at 350 °C for 3 h as a standard pretreatment followed by cooling down to the reaction temperature to 100 °C. The reactive and products of the reaction were analyzed in a Varian CP-3800 gas chromatograph equipped with CTR1 6'columns Porapak Q 80 -100 mesh 2,5m.

3. Results and discussion

3.1. Hydrotalcites characterization

X-ray diffraction patterns of the uncalcined solids (Fig. 1) showed the typical diffractograms of hydrotalcite-like materials (JCPDS 14-191). The sharp and intense peaks at $2\theta \approx 11°$, 23°, and 34° correspond to the (0 0 3), (0 0 6), and (0 0 9) planes, indicating a well-formed crystalline layered structure with a rhombohedral

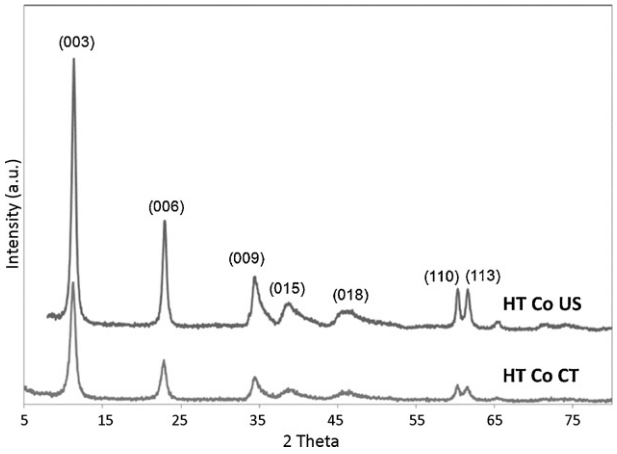

Fig. 1. Powder X-ray diffraction patterns of hydrotalcite samples depending of aging treatment.

Table 1
Lattice parameters *a* and *c* and textural properties of hydrotalcites.

Solid	Lattice parameters		BET ($m^2\ g^{-1}$)	Pore volume ($cm^3\ g^{-1}$)
	a (nm)	*c* (nm)		
HT Co CT	0.3063	2.351	61	0.2317
HT Co US	0.3065	2.346	83	0.3372

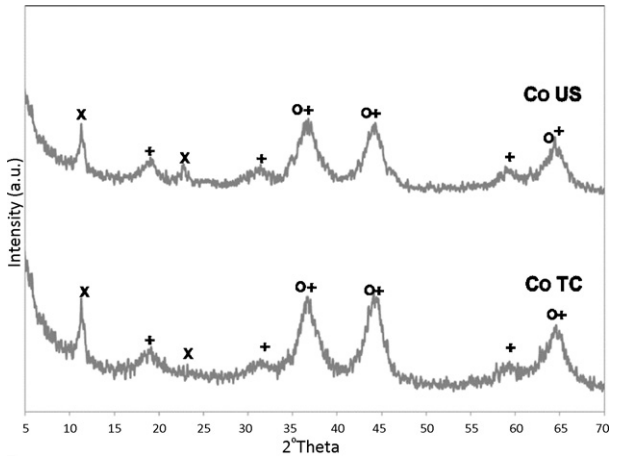

Fig. 2. Powder X-ray diffraction patterns of mixed oxides with conventional and ultrasound treatment x: HT; +:Co_3O_4; O: Periclase.

Table 2
Textural and redox properties of mixed oxides.

Solid	BET (m^2/g)	Pore volume (cm^3/g)	H_2 consumption		Total O_2 uptake (cm^3/g) STP
			Zone I (mmol/g)	Zone II (mmol/g)	
MOCo CT	164	0.2209	0.0849	0.3854	18.6
MOCo US	201	0.4552	0.1296	0.5129	25.3

symmetry (3R). It is remarkable that the use of ultrasound, allows hydrotalcite synthesis in much less time. Then the use of ultrasonic treatment for the hydrotalcite synthesis seems to be suitable. The cell parameters were calculated assuming a 3R polytype with a hexagonal cell [10,22], taking into account the positions of the peaks due to diffraction by the (0 0 3) plane to determine the *c* parameter, $c = 3d(0\,0\,3)$; and the position of the (1 1 0) reflection to calculate the *a* parameter, $a = 2d(1\,1\,0)$; the values are included in Table 1. No remarkable differences were observed between *c* parameters whatever the aging treatment given to the samples. Following the same trend, the values for the *a* parameter were almost constant, 3.06 Å, characteristic of the molar ratio 3 in the starting solutions ($M^{2+}/M^{3+} = 3$). It should be noted that when the ultrasound is used narrow and symmetric diffraction lines are observed, suggesting an improvement of the sample crystallinity. Based on evaluated FWHM values, the hydrotalcite crystallinity was significantly improved by ultrasound treatment. In general, the acoustic effect in the solid Co US allows having a lower FWHM value ($FWHM_{0\,0\,1} = 0.614^\circ$) than the solid with conventional treatment ($FWHM_{0\,0\,1} = 0.813^\circ$).

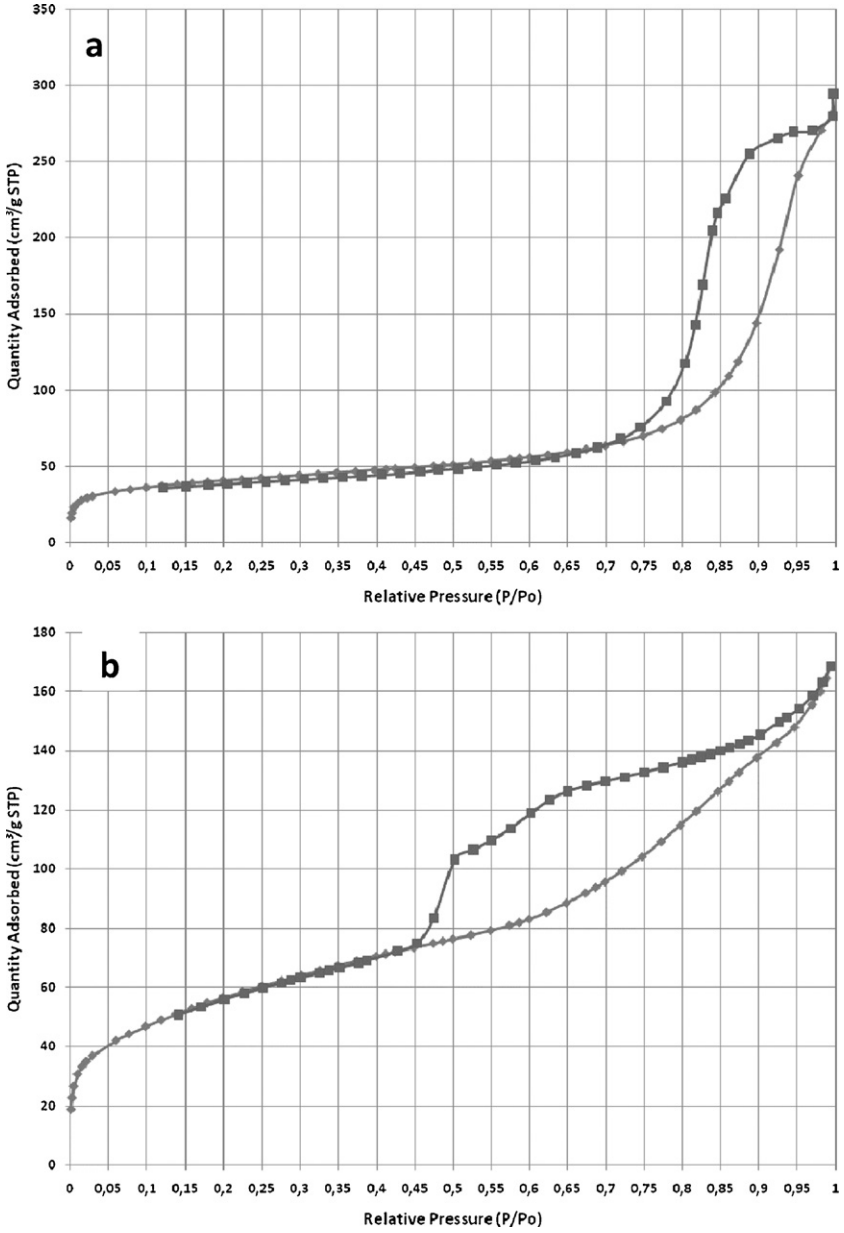

Fig. 3. N_2 adsorption/desorption isotherms of mixed oxides. (a) MOCo CT and (b) MOCo US.

The nitrogen adsorption/desorption behaviour of the hydrotalcites samples is reported. In both cases, the nitrogen sorption follows an isotherm of type IIb, according to the classification proposed by Rouquerol et al. [31], and a H3-type hysteresis loop for the desorption. Comparatively to the type IV, the isotherms of type IIb do not present a plateau at high P/P^0 values, and the clay minerals adopt generally these characteristics (anionic clays) [32,33]. The curve shape comes from nitrogen physisorption taking place between the aggregates of particles, and the closing of the desorption part is accompanied by a pronounced decrease in the adsorbed volume (at a relative pressure P/P^0 0.45). This corresponds to the filling of small mesopores [31].

The hydrotalcite prepared with ultrasound exhibits greater textural properties. Indeed the specific surface area of HTCoUS (83 m^2/g) is higher than that of HTCoCT (61 m^2/g) and the pore volume increase from 0.232 $cm^3\ g^{-1}$ for HTCoCT to 0.337 $cm^3\ g^{-1}$ for HTCoUS). Similar results have been observed on Mg–Al hydrotalcite by Kovanda et al. [34].

3.2. Mixed oxides characterization

When the samples are calcined, all the X-ray diffraction patterns turn out to be similar (Fig. 2), a small amount of hydrotalcite remains and broad peaks are present.

The diffractograms do not show signals corresponding to crystalline phases of aluminum oxide (Al_2O_3), suggesting that Al is in an amorphous phase and/or is part of the lattice with Co and Mg. The aluminum incorporation in solid solution with Mg, depends on the calcination temperatures and the relationship M^{2+}/M^{3+}. As such, it has been reported that hydrotalcites of Mg–Al relationships $M^{2+}/M^{3+} = 3$ (same as used in this study) where at temperatures below 1000 °C the Al forms homogeneously the structure of MgO, while at higher temperatures the Al changes from octahedral to tetrahedral to form the spinel structure. Similarly, the XRD indicated the presence of the hydrotalcite phase (after calcination). This result can be explained by the solid exposition of the atmosphere and the consequently the possible reconstruction of the hydrotalcite in the presence of water and CO_2. This effect is more noticeable in the case of solids with content Mg due to their growing tendency to carbonation.

The broadness of diffraction peaks can be also explained by the presence of a mixture of three oxide spinel phases very difficult to differentiate by XRD [20]: Co_3O_4 (JCPDS 421467), $CoAl_2O_4$ (JCPDS 440160) and Co_2AlO_4 (JCPDS 380814).

The specific surface area, pore volume and average pore diameter of mixed oxides are presented in Table 2.

The N_2 isotherms (Fig. 3) were of type IV for the two samples, typical of mesoporous materials, with the hysteresis loop associated with capillary condensation in the mesopores. The hysteresis type showed that the aggregates of plate-like particles formed non uniform slit shaped pores [33]. For the sample with ultrasound treatment (US), there was a significant difference in the isotherm shape at high relative pressures ($P/P^0 > 0.45$) showing ultrasound also changed the shape and/or size of the pores.

The samples with a conventional treatment (24 h) have a lower specific surface area than the sample of US treatment. It should be taken into account that, the CT sample was submitted, after coprecipitation, to an aging time of 24 h at 333 K, which prolongs the crystallization process and produces a decrease of the surface area of the mixed oxide obtained by calcination.

Thus, ultrasound not only accelerated the crystal formation but dispersed small particles as well as it reduced the aggregation during nucleation and crystal growth, giving rise to a large increase in the specific surface area.

Fig. 4 shows that the average pore size consistently decreased with ultrasound treatment. The sample with ultrasound exhibited

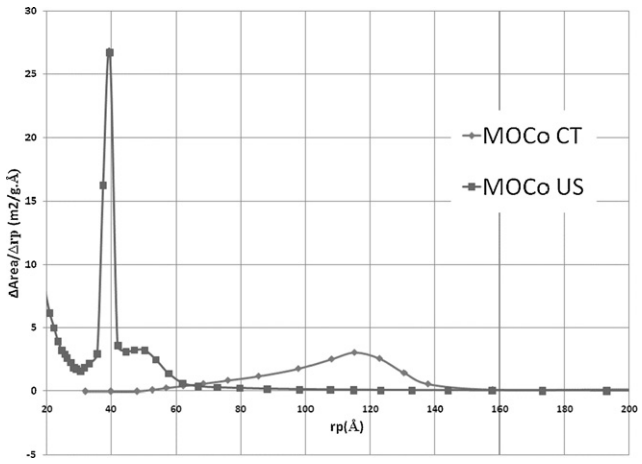

Fig. 4. Pore size distributions for mixed oxides conventional and ultrasound treatment.

the most narrow pore size distribution, whereas the distributions patterns for conventional treatment were much broader. This suggests that hydrotalcite treated with ultrasound was more uniformly packed together compared to hydrotalcite treated for 24 h. Hydrotalcite with ultrasound could be selected for use as support due to its narrow pore size distribution.

TPR patterns of mixed oxides are shown in Fig. 5. The H_2 consumption (Table 2) can be assigned to the reduction of cobalt species since Mg–Al mixed oxide is not easily reduced in the studied temperature range. Reduction of the both samples proceeds in two steps with maxima at 398 °C and 935 °C for MOCo CT and 400 °C and 775 °C for MOCo US. The first peak can be attributed to the reduction of Co_3O_4: Co^{3+} ions are first reduced to Co^{2+} ions followed by reduction of Co^{2+} ions to metallic Co. The reduction of pure Co_3O_4 used as a reference sample takes place in the same temperature range (200–400 °C) [35]. The second peak is ascribed to reduction of the same species but in Co–Al spinel-type mixed oxide [36]. The use of ultrasonic treatment during the hydrotalcite modifies the redox properties of the corresponding mixed oxides because (i) a higher H_2 consumption is observed (Table 2) and (ii) a significant shift to lower temperature is observed for the high temperature reduction peak because the reduction temperature of cobalt species in Co–Al spinel-type mixed oxide is lowered of 800 °C. This could be explained considering a particle size effect, a smaller particle size imply a lower reduction temperature, as it could see in textu-

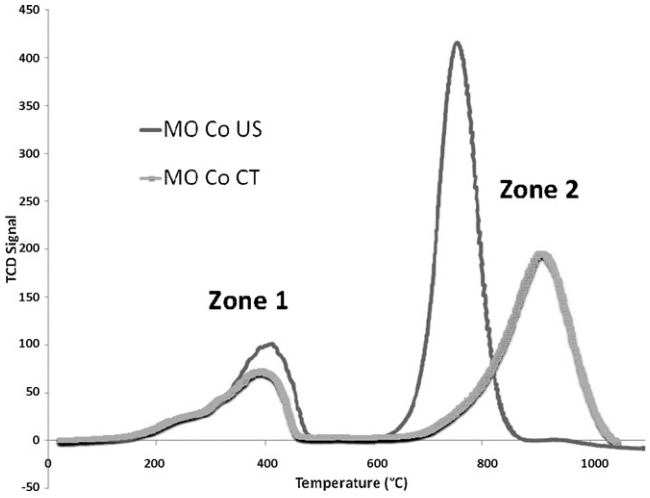

Fig. 5. TPR-H_2 for the mixed oxides: ultrasound effect.

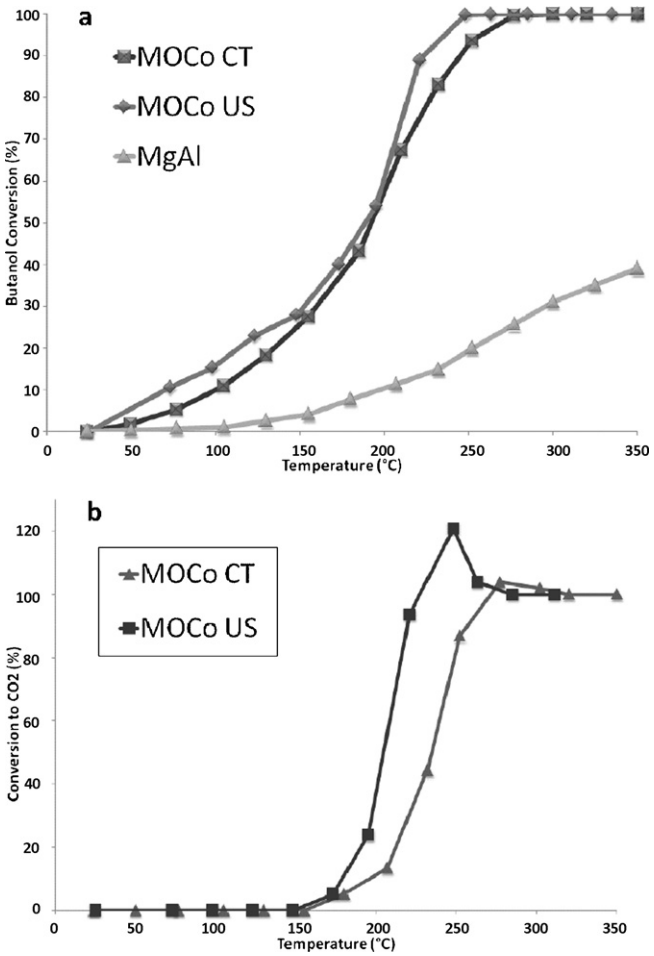

Fig. 6. (a) Butanol conversion versus temperature and (b) selectivity to CO_2 for the samples MOCo CT and MOCo US.

ral properties, a higher surface specific area value is obtained for MOCo UC, indicating probably the formation of smaller particles size in this sample. For the solid Co US, the total amount of hydrogen consumed during the reduction is higher comparing to the conventional treatment also, the T_M for the solid is located at low temperatures allowing to have cobalt species which are involved in the reaction at lower temperatures more disposed.

The TPO profiles of the mixed oxides of cobalt present only one peak at 308 °C which is assigned to the oxidation of Co^{2+} at Co^{3+} [37,38]. Furthermore it appears that the mixed oxide obtained from the hydrotalcite synthesized by applying ultrasounds, the oxygen storage are higher than the hydrotalcite prepared by a conventional procedure (Table 2).

Oxygen storage capacity increase as well as specific surface area and H_2 consumption enhancement is respectively observed from TPO, SBET and TPR-H_2 measurements, result that are directly related to a good dispersion of metals on calcined solids.

3.3. Catalytic test

It is first noticeable in Fig. 6a is that the oxide obtained from the simple hydrotalcite (only Mg–Al) presents low catalytic activity, being that it does not contain potentially active sites for oxidation and the conversion of 27% at 300 °C can be subject possibly to thermal effects involved in the reaction or the intrinsic basic properties that the Mg could has in the material.

It can be observed in Fig. 6a the effect of the presence of cobalt in the hydrotalcite to obtain more active oxides, result that indicates a beneficial effect by the incorporation of this metal. Also, the effect of ultrasound on the solid with cobalt is showed. The catalytic activity of the mixed oxide MOCo US is slightly better. These results clearly show that, as can be expected, the total number of active sites increases when increasing the oxygen storage of the solid. Also, H_2 consumption could describe the best activity showed by ultrasound treatment; the zone at lower temperatures (150–450 °C) corresponds to the range of temperature in which the catalytic test is carried out and where a higher H_2 consumption is associated to a better catalytic activity.

Table 3
Parameters for evaluating the total oxidation of butanol.

Solid	$T_{50\%}$ conv.	% Butanal	T CO_2[a]
MOCo CT	189	12	178
MOCo US	189	7	169

[a] Starting temperature in the production to CO_2.

The selectivity curves to CO_2 for MOCo CT and MOCo US catalysts have been included in Fig. 6b. As it can been seen a remarkable conversion calculated from the CO_2 signal for the solid with ultrasound sample reaches approximately 120% at 250 °C. This result is directly related to the adsorption of CO_2 and the VOC on the catalyst surface [39] and may be accounted for by the fact that there is a better dispersed cobalt on the surface as result from ultrasound treatment as it could be inferred by the specific surface area results, which is in line with the best activity towards the oxidation of butanol.

The solid with ultrasound present lower selectivity to butanal (Table 3), revealing a greater selectivity to total oxidation towards CO_2 and H_2O. From these results, it is evident that the hydrotalcites used as precursors for the obtaining of mixed oxides and making use of ultrasound as a method of aging, obtaining excellent catalysts in oxidation reactions of VOCs.

4. Conclusion

The characterizations confirm the success of the synthesis of hydrotalcites as precursors of mixed oxides using ultrasound as an aging method, given the same structural properties and in some cases, have improved allowing solids with better characteristics in only 10 min of treatment time in comparison with those reached during the conventional 24 h treatments. The hydrotalcites used as precursors for the obtaining of mixed solids are excellent catalysts in the oxidation reactions of COVs with high selectivity towards products of total combustion, showing that ultrasound is an effective and novel technique to get solids with better catalytic properties.

Acknowledgement

This work is financially supported by an ECOS-Nord (France) and Colciencias (Colombia) program Action n° C09P02.

References

[1] O.E. Lebedeva, A.G. Sarmurzina, Applied Catalysis B: Environmental 26 (2000) L1.
[2] D. Delimaris, T. Ioannides, Applied Catalysis B: Environmental 89 (2009) 295.
[3] K. Everaert, J. Baeyens, Journal of Hazardous Materials 109 (2004) 113.
[4] J. Tsou, P. Magnoux, M. Guisnet, J.J.M. Órfão, J.L. Figueiredo, Applied Catalysis B: Environmental 57 (2005) 117.
[5] D. Aguilera, A. Perez, R. Molina, S. Moreno, Studies in Surface Science and Catalysis 175 (2010) 513.
[6] W.B. Li, W.B. Chu, M. Zhuang, J. Hua, Catalysis Today 93–95 (2004) 205.
[7] L. Wang, M. Sakurai, H. Kameyama, Journal of Hazardous Materials 154 (2008) 390.
[8] A. Musialik-Piotrowska, H. Landmesser, Catalysis Today 137 (2008) 357.

[9] H.L. Tidahy, S. Siffert, J.F. Lamonier, E.A. Zhilinskaya, A. Aboukaïs, Z.Y. Yuan, A. Vantomme, B.L. Su, X. Canet, G. De Weireld, M. Frère, T.B. N'Guyen, J.M. Giraudon, G. Leclercq, Applied Catalysis A: General 310 (2006) 61.
[10] K. Jirátová, J. Mikulová, J. Klempa, T. Grygar, Z. Bastl, F. Kovanda, Applied Catalysis A: General 361 (2009) 106.
[11] B. Levasseur, S. Kaliaguine, Applied Catalysis B: Environmental 88 (2009) 305.
[12] D. Delimaris, T. Ioannides, Applied Catalysis B: Environmental 84 (2008) 303.
[13] J. Carpentier, S. Siffert, J. Lamonier, H. Laversin, A. Aboukaïs, Journal of Porous Materials 14 (2007) 103.
[14] J. Cervený, J. Splíchalová, P. Kacer, F. Kovanda, M. Kuzma, L. Cervený, Journal of Molecular Catalysis A: Chemical 285 (2008) 150.
[15] D. Tichit, D. Lutic, B. Coq, R. Durand, R. Teissier, Journal of Catalysis 219 (2003) 167.
[16] S. Ribet, D. Tichit, B. Coq, B. Ducourant, F. Morato, Journal of Solid State Chemistry 142 (1999) 382.
[17] M.R. Othman, N.M. Rasid, W.J.N. Fernando, Chemical Engineering Science 61 (2006) 1555.
[18] J.A. Rivera, G. Fetter, P. Bosch, Microporous and Mesoporous Materials 89 (2006) 306.
[19] K.S. Chang, H. Song, Y.-S. Park, J.-W. Woo, Applied Catalysis A: General 273 (2004) 223.
[20] S. Kannan, Applied Clay Science 13 (1998) 347.
[21] J.J. Yu, J. Cheng, C.Y. Ma, H.L. Wang, L.D. Li, Z.P. Hao, Z.P. Xu, Journal of Colloid and Interface Science 333 (2009) 423.
[22] S. Albertazzi, F. Basile, A. Vaccari, W. Fernando, S. Kestur Gundappa, Interface Science and Technology, vol. 1, Elsevier, 2004, p. 496.
[23] G. Centi, S. Perathoner, Applied Catalysis B: Environmental 70 (2007) 172.
[24] C. Gennequin, R. Cousin, J.F. Lamonier, S. Siffert, A. Aboukaïs, Catalysis Communications 9 (2008) 1639.
[25] J. Carpentier, J.F. Lamonier, S. Siffert, E.A. Zhilinskaya, A. Aboukaïs, Applied Catalysis A: General 234 (2002) 91.
[26] C. Gennequin, S. Kouassi, L. Tidahy, R. Cousin, J.-F. Lamonier, G. Garcon, P. Shirali, F. Cazier, A. Aboukaïs, S. Siffert, Comptes Rendus Chimie 13 (2010) 494.
[27] J. Quiroz-Torres, R. Averlant, J.-M. Giraudon, J.-F. Lamonier, Studies in Surface Science and Catalysis 175 (2010) 517.
[28] W.N. Budhysutanto, H.J.M. Kramer, D. van Agterveld, A.G. Talma, P.J. Jansens, Chemical Engineering Research and Design 88 (2010) 1445.
[29] M. Mokhtar, T.S. Saleh, N.S. Ahmed, S.A. Al-Thabaiti, R.A. Al-Shareef, Ultrasonics Sonochemistry 18 (2011) 172.
[30] C.E. Daza, J. Gallego, J.A. Moreno, F. Mondragón, S. Moreno, R. Molina, Catalysis Today 133–135 (2008) 357.
[31] J. Rouquerol, F. Rouquerol, Y. Grillet, R. Denoyel, Thermochimica Acta 148 (1989) 183.
[32] D. Tichit, O. Lorret, B. Coq, F. Prinetto, G. Ghiotti, Microporous and Mesoporous Materials 80 (2005) 213.
[33] E.M. Sabbar, M.E. de Roy, F. Leroux, Microporous and Mesoporous Materials 103 (2007) 134.
[34] F. Kovanda, D. Kolousek, Z. Cílová, V. Hulínský, Applied Clay Science 28 (2005) 101.
[35] G. Bagnasco, C. Cammarano, M. Turco, S. Esposito, A. Aronne, P. Pernice, Thermochimica Acta 471 (2008) 51.
[36] B. Coq, D. Tichit, S. Ribet, Journal of Catalysis 189 (2000) 117.
[37] B. Zapata, P. Bosch, G. Fetter, M.A. Valenzuela, J. Navarrete, V.H. Lara, International Journal of Inorganic Materials 3 (2001) 23.
[38] F. Basile, P. Benito, G. Fornasari, A. Vaccari, Applied Clay Science 48 (2010) 250.
[39] M. Paulis, L.M. Gandía, A. Gil, J. Sambeth, J.A. Odriozola, M. Montes, Applied Catalysis B: Environmental 26 (2000) 37.